Accuracy Evaluation Orthorectification of SPOT Image

Sarip Apip Hidayat
Data Services Division
Remote Sensing Ground Station
Pare Pare,Indonesia
sarip.hidayat@lapan.go.id

Wiweka
Environmental and Mitigation Disaster Division
Application Remote Sensing Center
Jakarta, Indonesia
wiweka@lapan.go.id

Abstract**—** Orthorectification in the study conducted on 14 scene multispectral imagery SPOT4 SPOT2 and West Java. The composition of the scene to form a wide block with no gaps, making it possible to do block triangulation. This triangulation is used to determine the relationship between the satellite image and the earth. The information generated from the triangulation will be used as input during orthorectification. Ground control points (GCP) were taken from the data vector Indonesian Topographic Map 1:25,000 scale and elevation data extracted from the DEM derived from contour maps RBI data is the same. Triangulation blocks performed with various configurations GCP and tie points (TP), the minimal configuration, just along perimemeter blocks, regularly spaced regularly spaced half scene and a third scene. Each configuration is lowered into several configurations based on the use of TP. Triangulation accuracy result was tested with 244 check points (CP) that spread in the block.Configuration can produce a minimum GCP accuracy RMSE (Root Mean Square Error) 1.25 pixels if equipped with a TP meeting. GCP configuration on the perimeter of the block is not recommended for use if it is not equipped with TP. Highest accuracy resulting from configuration GCP / TP per a third scene with RMSE 0.98 pixels. Accuracy will be determined by the distribution and the number of GCP and the use of TP. Best accuracy of this research is suitable for medium-scale map updates 1:65.000.
Keywords: orthorectification, SPOT, triangulation, accuracy

I. INTRODUCTION

Availability of satellite images SPOT (Systeme Pour l'Observation de la Terre) series 2/4 or SPOT2 / 4 of the territory of Indonesia is quite a lot and almost covers the entire region. Since 2006, SPOT receiving station on earth (Direct Receiving Station / DRS) SPOT2 / 4 Indonesia have started recording the satellite imagery. Satellite imagery product standards SPOT2 / 4 issued by DRS is to have claimed the 2A level horizontal accuracy to 350 m (1σ) (Spot Image, 2008). Observation capabilities oblique (oblique viewing) on HRV instrument SPOT2 / 4 can increase the frequency of imaging (revisit capability), as well as will lead to relief displacement errors in the elevation of the point object (Fig. 1). Relief displacement occurs if the points are located at the same coordinates but different horizonzal elevation, for example, between the top and base of the building, was described in different locations in the image [13]

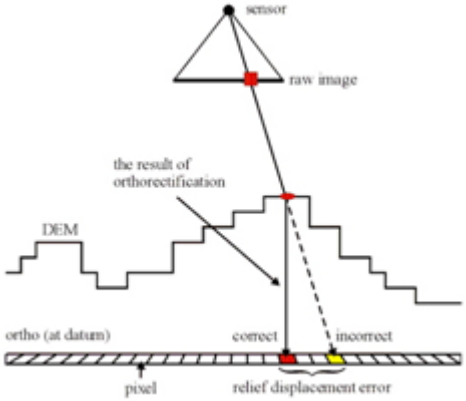

Fig. 1 Illustration orthorectification of imagery using sensor geometry model and DEM (PCI Geomatics, 2006)

Satellite remote sensing can fly higher and more stable, so that interference with the satellite orbit and behavioral changes are relatively small vehicle. This condition can provide the opportunity to effectively eliminate distortion [24]. Photogrammetric triangulation techniques to approach the block (block triangulation) can eliminate the distortion in satellite imagery more efficiently and produce reliable ortho imagery.

The purpose of research is to improve the accuracy of image SPOT2 / 4 through orthorectification, the initial hypothesis that the bloc satellite image orthorectification generated by pushbroom scanner, can be done with the results of triangulation control points and satellite imagery will produce high accuracy with the minimum number of control points.

II. METHODOLOGY

The image is taken from SPOT2 and SPOT4 that both have similar characteristics. To maintain the geometric conditions as the original image from the CCD and have not experienced any geometric correction, the image used SPOT2 / 4 level 1A (Fig. 2). Channel is used without panchromatic multispectral spatial resolution of 20 m. The image has a variety of angles of observation, started almost straight up to almost maximum tilt. Image block covers an area of West Java, which has a

large variation in elevation, ranging from lowlands to hilly and mountainous

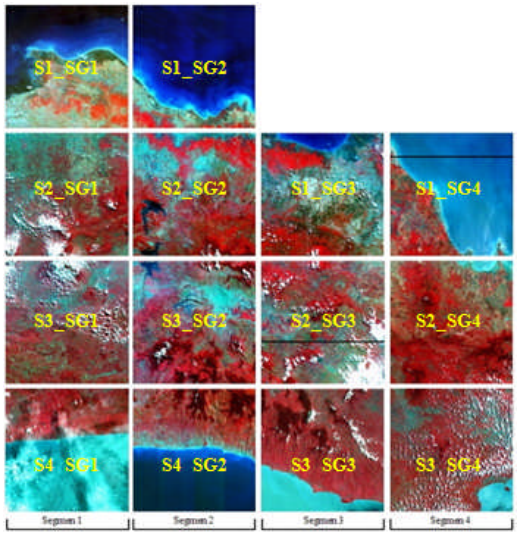

Fig. 2 Quicklook SPOT imagery XI / XS 1A level in four segments arranged to form an image and image blocks without gap

A. Mathematical Models of Satellite Orbit

Triangulation of satellite imagery in this study using a Satellite Orbital Math Model, developed by Dr.. Toutin at the Canada Centre for Remote Sensing (CCRS). This model uses the principle of equal collinear (collinearity equations), to calculate the mathematical relationship between image, sensor and earth (Fig. 3). This model is included in the software PCI Geomatica V10.0.3 OrthoEngine and requires information to complete an orbit, and the whole scene that has never been experienced geometric processing. Collinear equations to satellite images generated by pushbroom scanner written in equation 1.

$$0 = -f \left[\frac{m_{21x}\left(X_A - X_{Lx}\right) + m_{22x}\left(Y_A + Y_{Lx}\right) + m_{13x}\left(Z_A + Z_{Lx}\right)}{m_{31x}\left(X_A - X_{Lx}\right) + m_{32x}\left(Y_A + Y_{Lx}\right) + m_{33x}\left(Z_A + Z_{Lx}\right)} \right] \quad (1)$$

$$y_a = y_o - f \left[\frac{m_{21x}\left(X_A - X_{Lx}\right) + m_{22x}\left(Y_A + Y_{Lx}\right) + m_{13x}\left(Z_A + Z_{Lx}\right)}{m_{31x}\left(X_A - X_{Lx}\right) + m_{32x}\left(Y_A + Y_{Lx}\right) + m_{33x}\left(Z_A + Z_{Lx}\right)} \right] \quad (1)$$

Where y_a are the coordinates y (column number) in the image to the point A; y_o are the coordinates y on the line for the image focal point; f is the focal length of the sensor; m_{11x} until m_{33x} is a component of the matrix rotation for orientation sensor when the line x_a acquired; X_{Lx}, Y_{Lx}, and Z_{Lx} are the coordinates of the sensor when the line x_a acquired; X_A, Y_A, and Z_A are the coordinates of the point object A

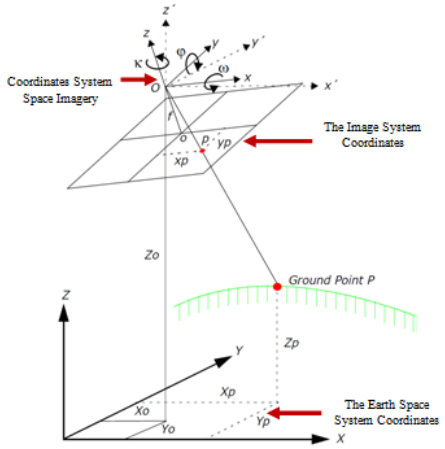

Fig. 3 Elements external orientation (Leica Geosystems, 2005)

Pushbroom scanners perform scanning along a scan line (scan line). Scanner continues to move along the satellite track (vehicle trajectory) and the sweep of line image (Fig. 4). So a scene SPOT image acquired from many points of exposure. For each scan line has a central perspective and a unique rotation angle (orientation elements outside). By the time the satellite moves from one scan line to the next scan line, then the external orientation elements changed

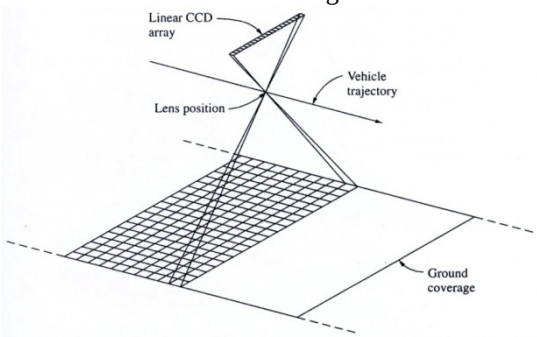

Fig. 4 Geometry imaging using linear array sensor [21]

One scene SPOT imagery XI / XS 3000 rows of pixels arranged and each line has 3000 pixels. Fig. 5 is an illustration of the scene SPOT image as a pushbroom scanner products, starting position (point o) is the projection of the center row 0 on earth. At this point, satellite sensors have a certain set of exterior orientation elements $\omega_0, \phi_0, \kappa_0, X_{L0}, Y_{L0}, Z_{L0}$

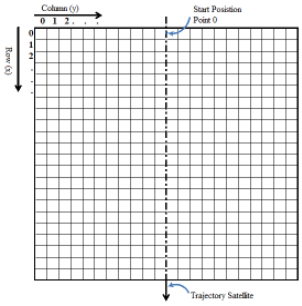

Fig. 5 Illustration of a scene image is generated from a linear sensor array [21]

Exterior orientation elements such variation is a function of the coordinates x (lines in the image). Due to the high level of stability during satellite imaging, the external orientation

elements can be assumed to vary in a systematic way. Exterior orientation variations on each line that can be modeled with low-order polynomial (equation 2) as described in [21].

$$\left.\begin{aligned} \omega_x &= \omega_o + a_1 x \\ \phi_x &= \phi_o + a_2 x \\ \kappa_x &= \kappa_0 + a_3 x \\ X_{L_x} &= X_{L_o} + a_4 x \\ Y_{L_x} &= Y_{L_o} + a_5 x \\ Z_{L_x} &= Z_{L_o} + a_6 x + a_7 x^2 \end{aligned}\right\} \qquad (2)$$

Where x is the number of lines of the image position; ω_x, φ_x, κ_x, X_{Lx}, Y_{Lx} and Z_{Lx} is an element of external orientation of the sensor when the line x obtained; ω_0, φ_0, κ_0, X_{Lo}, Y_{Lo} and Z_{Lo} is an element of external orientation sensor on the starting position; a_1 until a_7 is a coefficient that describes the systematic variation of external orientation elements at the time the image was acquired

B. Implementation Procedures Triangulation

Activities began with the preparation of maps and imagery, image pretreatment, the determination of the configuration of GCP / TP and CP, then processed by the triangulation of satellite imagery and the final stage is the analysis of the precision, accuracy and image quality as well as the suitability of ortho-scale map is generated.

In the pretreatment images do image reconstruction and grafting SPOT level 1A (stitch) scene. Reconstruction aims to rebuild the image SPOT2 / 4 level 1A of Dimap format into a format PCIDSK Geomatica 10.0.3, by adding segments that contain data binary orbit (ephemeris) into the image. While working to reconnect stitch multiple images at the scene of the segment that has the same date of acquisition. In this stage also the identification and marking of the CP to be used in assessing the quality of the results of the 1A level image reconstruction. Flowchart of the implementation of the triangulation procedure is presented in Fig. 6.

Implementation of triangulation block a few times in accordance with the design configuration of GCP / TP. Identification and marking of GCP / TP is a critical job, in which the results will determine the quality of the triangulation. Therefore GCP quality must be controlled so that it has a high precision and error free blunder. Configuration GCP / TP is in the form of setting the amount, distribution and use of a combination of GCP and TP. Determination of the number of GCP GCP is based on a consideration of the minimum amount, regularity and regularity distance between GCP GCP distribution on the whole block. Configuration GCP / TP is used in the block triangulation experiments described in Fig. 7.

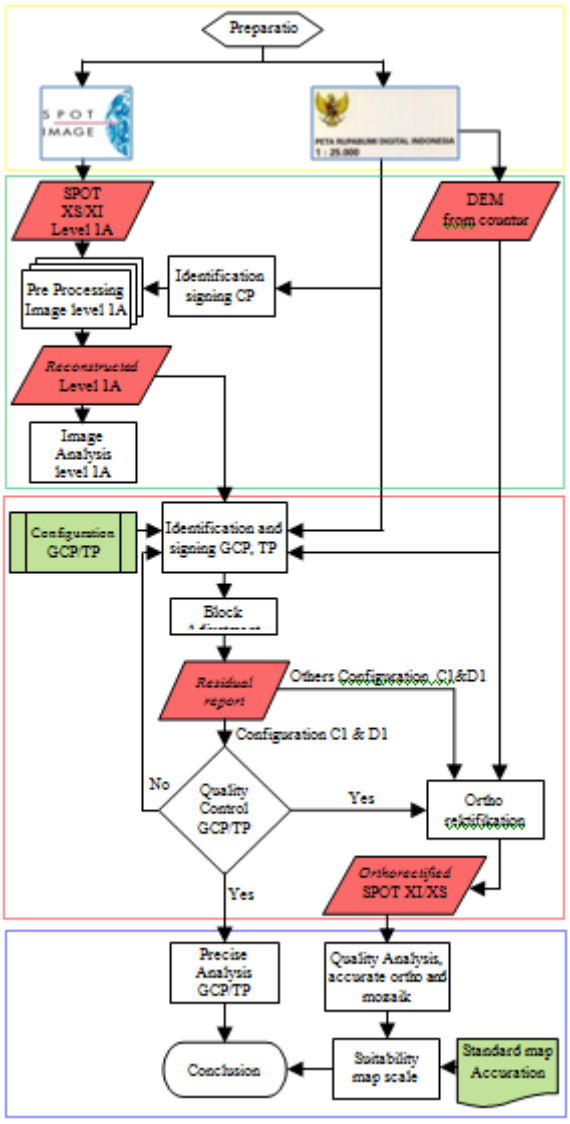

Fig. 6 Flow chart of the study

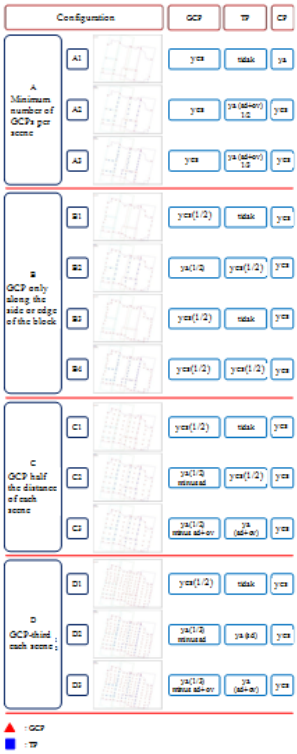

Fig. 7 Configuration experiment GCP / TP

C.Ortho Image Production

The approach used in constructing ortho imagery is a forward projection (Fig. 8). The pixels of the original image (the image still contains a perspective projection) is projected to DEM to obtain the object space coordinates to pixel in question. Object space coordinates are then projected into the grid ortho imagery. The second projection this time while transferring the digital value of the original image and will generate an irregular arrangement of pixels on the image ortho. Irregularity of the pixel array is affected by variations in elevation and the effect of perspective projection. To reconstruct the pixels into a regular, then the interpolation (resampling) the ortho image formed [13]

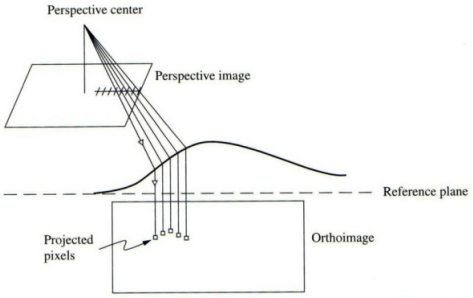

Fig. 8 Illustration of the process of formation of ortho imagery using forward projection (Mikhail, 2001)

Accuracy ortho imagery expressed in RMSE CP, ie the square root of the average squared residual or discrepancy (EC-JRC Ispra, 2008). RMSE can be calculated by the following equation distance (FGDC-STD-007, 1998):

$$RMSE = \sqrt{\frac{1}{n}\sum_{i=1}^{n}[(x_r - x_i)^2 + (y_r - y_i)^2]} \quad (3)$$

Where x_r and y_r are the coordinates of the coordinate input or reference; x_i and y_i are the coordinates of the coordinate transformation result or calculation result, n the number of points (CP, GCP or TP) and i is an integer from 1 to n.

III. Result And Analysis

A. Results 1A Level Image Reconstruction

Image generated from this process will have a geometry as in the time of acquisition. Scene size, shape and spatial resolution imagery scene will change according to the character of the imaging geometry of the scene in question. All scene images will be tilted to the east because the scene was acquired during orbit down (descending node) and due to the rotation of the earth from west to east, as shown in Fig. 9.

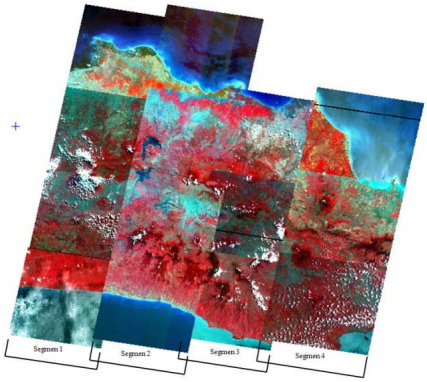

Fig. 9 Cita 1A level using the reconstructed orbit data from metadata, visible all the scene has been tilted to the east and the size of the scene is not the same

In Table 1 there is a trend to greater entry angle (incidence angle), the greater the spatial resolution at the East-West direction (X direction), while the North-South direction (Y direction) is relatively fixed. Large entry angle will potentially cause a shift in the location of areas with large elevation.

Table 1
Difference in spatial resolution at the level 1A image reconstruction results

No.	*Scene-id*	Satellite	Reconstruction Level	Mode	Angle	Total Pixel	Spatial Resolution (dX x dY) m
1	S1SG1	SP4	1A	XI	R 2,5	3.000 x 3.000	19,96 x 20,06
2	S2SG1	SP4	1A	XI	R 2,5	3.000 x 3.000	19,96 x 20,05
3	S3SG1	SP4	1A	XI	L 5,6	3.000 x 3.000	20,11 x 20,05
4	S4SG1	SP2	1A	XS	L 14,1	3.000 x 3.000	21,04 x 20,04
5	S1SG2	SP2	1A	XS	L 17,9	3.000 x 3.000	21,86 x 20,04
6	S2SG2	SP2	1A	XS	L 17,9	3.000 x 3.000	21,86 x 20,04
7	S3SG2	SP2	1A	XS	L 17,9	3.000 x 3.000	21,77 x 20,04
8	S4SG2	SP2	1A	XS	L 17,9	3.000 x 3.000	21,67 x 20,03
9	S1SG3	SP2	1A	XS	R 2,2	3.000 x 3.000	19,94 x 20,08
10	S2SG3	SP2	1A	XS	R 2,2	3.000 x 3.000	19,93 x 20,06
11	S3SG3	SP4	1A	XI	L 28,6	3.000 x 3.000	25,63 x 20,00
12	S1SG4	SP2	1A	XS	L 25,8	3.000 x 3.000	24,22 x 20,04
13	S2SG4	SP2	1A	XS	L 25,8	3.000 x 3.000	24,24 x 20,04
14	S3SG4	SP2	1A	XS	L 25,8	3.000 x 3.000	24,31 x 20,03

B. *Shifting pixels on the detector Pushbroom*

Shift the location of points on the pushbroom detector can be caused by the change in magnitude and the angle of observation object height variation. To determine the pixel shift in pushbroom detector, the simulation geometry SPOT imagery at the viewing (viewing angle) and the height of different objects. Simulation results are presented in Fig. 10, which shows that it is theoretically occur if the pixel shift observations by satellite sensor at an angle to the nadir and the observed object has a different elevation.

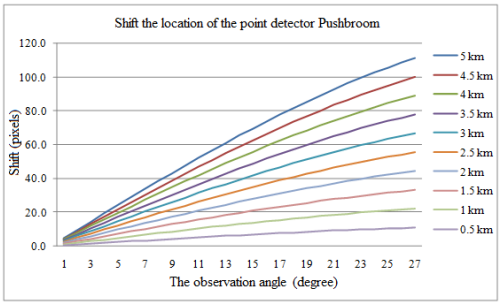

Fig. 10 Shifting the location of the simulation results at different elevations points (objects) and the observation angle variation

C. *Accuracy Level 1A Reconstruction Results*

Accuracy was tested with 244 CP and RMSE are expressed in pixels. Every scene looks still have a good geometric distortions in the X direction and in the direction Y. In general, the accuracy level is still low and lower than SpotImage claim is better than 350 m. Theoretically, if the angle of the entrance to the area with large elevation would have a big X residue, but has no effect on a relatively flat area. In general, visible residues on the flat area is always lower than areas with high elevation and the greater the angle the greater it will go residues in the X direction (Fig. 11). While the trend in the Y direction is not entirely true, residues in Y direction is not always influenced by the incoming angle and elevation, but is more affected by a disturbance in the orbit. For example, the image of the entrance angle 2.2^0, has a direction Y residues greater than the image that has a corner entrance 28.6^0

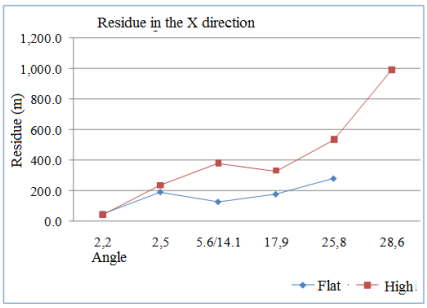

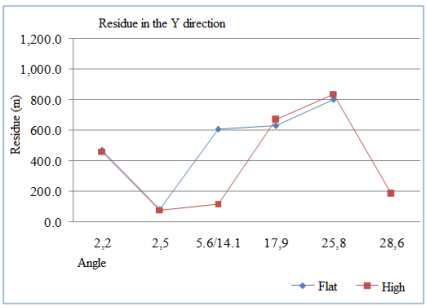

Fig. 11 residues X and Y direction on a flat area and height for the image reconstruction results SPOT level 1A

D. *Scene Image Splicing Results (Stitch)*

Results splicing of two or more image scene will establish a long scene (strip). The formation of the strip will help in working on projects with a number of images that a lot. Number of scenes to be processed is reduced so that the number of GCP can also be reduced. Another advantage is coverage for a scene to be longer, so as to bridge the areas that are not obvious, such as the area under the cloud cover in the area where they can not be taken GCP. Configuration is now a combination block and strip scene as shown in Fig. 12. Border connections will be connected with the scene perfectly and looks seamless. Strip image appears continuous, because the original image is constantly on the North - South. This scene is the process of switching image reconstruction 1A level, but on several scenes at once acquired

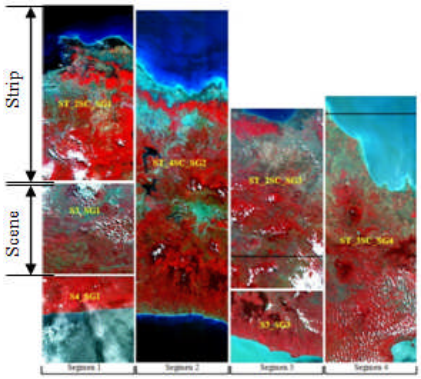

Fig. 12 Configuration 1A level combined image and single image strip

D. *GCP Quality*

Quality GCP (GCP precision) expressed with residues (in pixels) from the calculation of the mathematical model. GCP precision can be seen from the residual value and the sign (+ / -) in the direction of the X residue and residue toward Y. GCP quality in this study only tested the configurations C1 and D1 are indicated by the graph in Fig. 13.

After a blunder elimination, residues on both the configuration they are in the "bull's eye" and looks almost evenly on all four quadrants chart. The red circle in the chart is equal to 1 pixel RMSE tolerance. GCP and the adjacent residues are in a group in the "bull's eye" indicates that the GCP is used has the precision and consistent. If many observations made or point calculated to produce the same

quantity of residue is small, it is indicates a high precision as stated in [7]

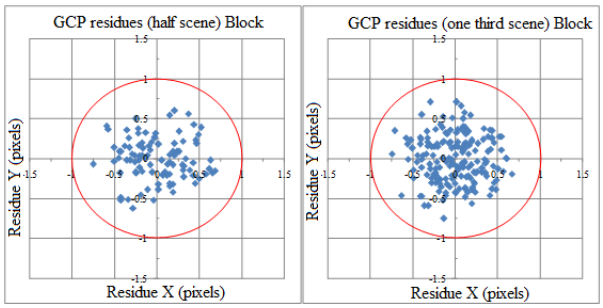

Fig. 13 residue X and residue Y for configuration C1 (left) and configuration D1 (right)

F. Quality Triangulation Result

Quality results expressed triangulation with an accuracy measured using the CP and the RMSE values expressed in pixels. CP in this study were drawn from the same map with the decision-GCP. The amount and distribution of CP on scene and strip does not change, so always use the same CP in different configurations. CP distribution in the block are presented in Fig. 14.

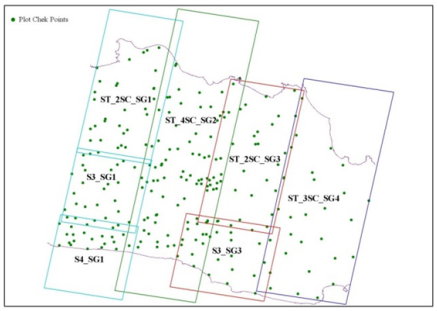

Fig. 14 Distribution of CP in the image block

In general, when arranged sequentially from configuration A to D, with the exception of configuration B1 and B3, looks higher accuracy (Table 2). In each configuration has the highest accuracy, ie the configuration of A3, B4, C3 and D3.

Table 2
Summary of Residue GCP / TP and CP RMSE on each configuration

Configuration		Σ GCP Total	Res-GCP (pixel)	Σ TP	Res-TP (pixel)	Σ CP	RMSE CP (pixel)
A	A1	16	0,27	N/A	N/A	244	1,76
	A2	16	0,32	17	1,07	244	1,28
	A3	16	0,32	32	0,67	244	1,25
B	B1	31	0,33	N/A	N/A	244	5,52
	B2	31	0,39	21	0,38	244	1,19
	B3	42	0,36	N/A	N/A	244	19,04
	B4	42	0,38	36	0,53	244	1,11
C	C1	65	0,42	N/A	N/A	244	1,11
	C2	48	0,39	18	0,44	244	1,12
	C3	45	0,37	21	0,41	244	1,11
D	D1	132	0,42	0	N/A	244	0,98
	D2	104	0,40	30	0,64	244	1,00
	D3	98	0,38	36	0,63	244	0,98

N/A: Not Available

1)Worst Configuration

B1 and B3 configuration produces a much lower accuracy than the other B configuration. GCPnya precision is still consistent with the reference map, showing that the accuracy is more affected by GCP distribution on the configuration. Configuration B1 and B3 are not using TP and GCP only scattered on the perimeter of the block with a distance of half a scene (B1) and a third scene (B3). Thus there is no control at all points in the middle of the block and the RMSE is located far from the GCP or are in the middle of the block as shown in Fig. 15 for configuration B3. RMSE magnitude of CP at each point indicated by the length of the error vector (error vector) (yellow line) as shown in Fig. 15 and Fig. 16.

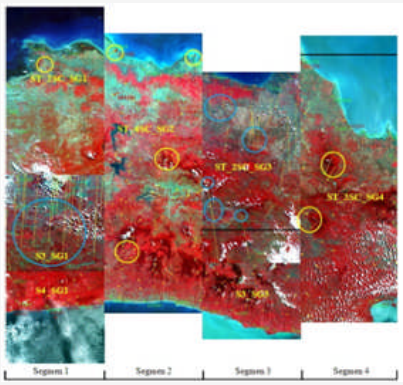

Fig. 15 Plot of the error vector (2500 times magnification digital) on the configuration B3, blue circle (O) indicates without subjectivity, while the yellow circle (O) shows the influence of the subjectivity

If the research will use the GCP configuration only on the perimeter, then at least there should be two sides of GCP on scene or strip to obtain good accuracy. This trend is seen in configurations B1 and B3 are only using the GCP on the perimeter of the block. When the image is composed by several blocks of image strips the same length as the strip ST_4SC_SG2, the GCP configuration fairly placed on the upper side and lower side only on each strip. GCP configuration as in ST_4SC_SG2 can produce good accuracy, it is similar to that reported in Tonon (2005). Accuracy in configuration B1 and B3 can be improved by adding TP to overlap / sidelap so its configuration changed to B2 and B4, RMSE value changes significantly as shown in Table 2. However, the C and D configurations, the use of TP to replace the GCP does not improve the accuracy significantly, as shown by the results of the variance ratio test.

2) Best configuration

Best configuration of this research is the D3 configuration. CP lowest RMSE value and use TP instead of GCP. Distribution of the error vector in block D3 for configuration is presented in Fig. 16. The solid line shows the RMSE error vector that is larger than one pixel. But Overall accuracy ortho imagery using D3 configuration produces less than one pixel RMSE

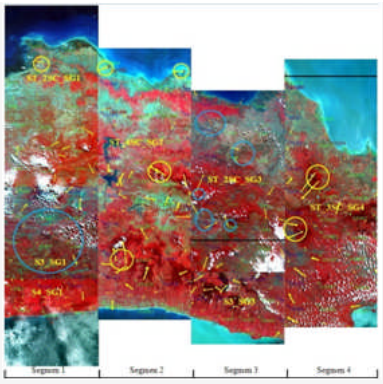

Fig. 16 Plot of the error vector (5000 times magnification digital) on the configuration of D3, blue circle (O) indicates without subjectivity, while the yellow circle (O) shows the influence of the subjectivity

3)Analysis of Variance Ratio

Variance ratio test is used to determine whether one configuration is better than the other configurations statistically. Used statistical distribution is the distribution of Fisher (F) with test statistic F = (S_1 ^ 2) / (S_2 ^ 2) [22], where the RMSE CP S_1 is the unity configuration and S_2 are RMSE CP of the second configuration . Tests conducted at the 90% confidence level or at the 0.1 significance level α. Conclusions can be drawn from these tests can be considered to choose the configuration that is better statistically. More variance ratio test results is presented in Table 3.

Table 3
The results of the variance ratio test RMSE CP

CONFIGURATION		GCP	TP	RMSE CP	Fisher's test
A-Minimal (The number of GCP at least 4 per image or per strip)	A1	(16)	N/A	1,76	
	A2	(16)	(17) sd+ov 1-2	1,28	
	A3	(16)	(32) sd+ov 1-3	1,25	
B-Perimeter (GCP only along side or edge block)	B1	(31) 1-2	N/A	5,52	
	B2	(31) 1-2	(21) sd+ov 1-2	1,19	
	B3	(42) 1-3	N/A	19,04	
	B4	(42) 1-3	(36) sd+ov 1-3	1,11	
C-Full (GCP each distance half the scene)	C1	(65) 1-2	N/A	1,11	
	C2	(48) 1-2	(18) sd 1-2	1,12	
	C3	(45) 1-2	(21) sd+ov 1-2	1,11	
D-Full (GCP each distance a third scene)	D1	(132) 1-3	N/A	0,98	
	D2	(104) 1-3	(30) sd 1-3	1,00	
	D3	(98) 1-3	(36) sd+ov 1-3	0,98	

The blue color on CP RMSE column shows the best configuration in a similar configuration. Orange line on the test column fisher Table 3 explains that the configurations are connected by the line did not produce statistically different variance at 90% confidence level. While configurations connected by colored lines violet explained that a better configuration than the configuration of the test pair.

F.Ortho Image Quality

Ortho imagery in this study was built with cubic convolution resampling method and sampling every single pixel spacing. Because rarely the same between the input image with a grid on the grid on the output image, the pixels must be processed gigital resampling to obtain a new value for the output image. The geometry of the image will change after a resampling process, as shown in Table 4. At the reconstruction level 1A SPOT imagery has a number of pixels (columns x rows) are the same in every scene that is 3,000 x 3,000 pixels, but has a spatial resolution varies depending on the angle of entry. After diresampling spatial resolution being 20 x 20 m, then the number of pixels will adjust to the spatial resolution.

Table 4
Changes in the geometry scene SPOT image reconstruction 1A level after experiencing a level ortho resampling

No.	*Scene ID*		Angle Entry	Level Reconstruction		Ortho level	
				Spatial Resolution (kolom x baris)	Spatial Resolution (dX x dY) m	Pixels Number (kolom x baris)	Spatial Resolution (dX x dY) m
1	ST_2SC_SG1	S1SG1	R 2,5	3.000 x 3.000	19,96 x 20,06	3.940 x 5.020	20 x 20
2		S2SG1	R 2,5	3.000 x 3.000	19,96 x 20,05		
3	S3SG1	S3SG1	L 5,6	3.000 x 3.000	20,11 x 20,05	3.650 x 3.410	20 x 20
4	S4SG1	S4SG1	L 14,1	3.000 x 3.000	21,04 x 20,04	3.420 x 1.570	20 x 20
5	ST_4SC_SG2	S1SG2	L 17,9	3.000 x 3.000	21,86 x 20,04	4.860 x 8.860	20 x 20
6		S2SG2	L 17,9	3.000 x 3.000	21,86 x 20,04		
7		S3SG2	L 17,9	3.000 x 3.000	21,77 x 20,04		
8		S4SG2	L 17,9	3.000 x 3.000	21,67 x 20,03		
9	ST_2SC_SG3	S1SG3	R 2,2	3.000 x 3.000	19,94 x 20,08	4.280 x 6.180	20 x 20
10		S2SG3	R 2,2	3.000 x 3.000	19,93 x 20,06		
11	S3SG3	S3SG3	L 28,6	3.000 x 3.000	25,63 x 20,00	4.170 x 3.320	20 x 20
12	ST_3SC_SG4	S1SG4	L 25,8	3.000 x 3.000	24,22 x 20,04	4.600 x 8.610	20 x 20
13		S2SG4	L 25,8	3.000 x 3.000	24,24 x 20,04		
14		S3SG4	L 25,8	3.000 x 3.000	24,31 x 20,03		

Fig. 17 is ortho imagery generated from D3 configuration. Some scenes appear to change shape, no longer rectangular or rhombus, but had to adjust the scope of DEM data are used. So in orthorectification to note that the coverage will be DEM data to determine the extent and form of image resampling results.

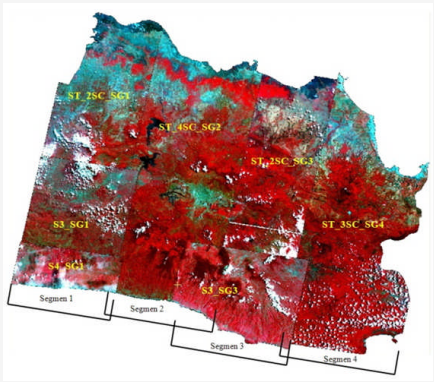

Fig. 17 Ortho image of showing the D3 configuration changes on the scene shape

The image that is outside the scope DEM will not undergo resampling, such as on the East side and West side ST_3SC_SG4 upper cut followed ST_2SC_SG1 visible perimeter DEM. Similarly, along the North Coast and South Coast of West Java will be cut, as part of the ocean does not have elevation data and only filled with the background value. While the image is within the scope of DEM resampling will be processed entirely, as in the scene S3_SG1 and all that is in the middle of the block.

Results cubic convolution resampling method of configuration kenampakkan D2 produces a smoother image (Fig. 18 (c)), although not as smooth as Fig. 18 (b). Excess Fig. 18 (c) is still revealing of detail that can be lost with bilinear interpolation method.

Fig. 18 (a) shows a great of detail, the value of the digital image does not change just to change position. But the elements are straight lines appear broken or jagged (jagged) so that the image appears dull or dirty. Fig. 18 (b) shows kenampakkan very subtle, but it looks fuzzy / blurry image of detail that can be lost, as the boundaries between the buildings and the streets are relatively small can disappear from the image.

The accuracy of the image of the cubic convolution resampling of the data vector 1:25:00 RBI shown in Fig. 19. Tumpangsusun visually look right with road and river vector data. Yellow stripes is the vector of the road and the river. Third resampling method would show similar accuracy, but cubic convolution method seems more appropriate approach vector lines.

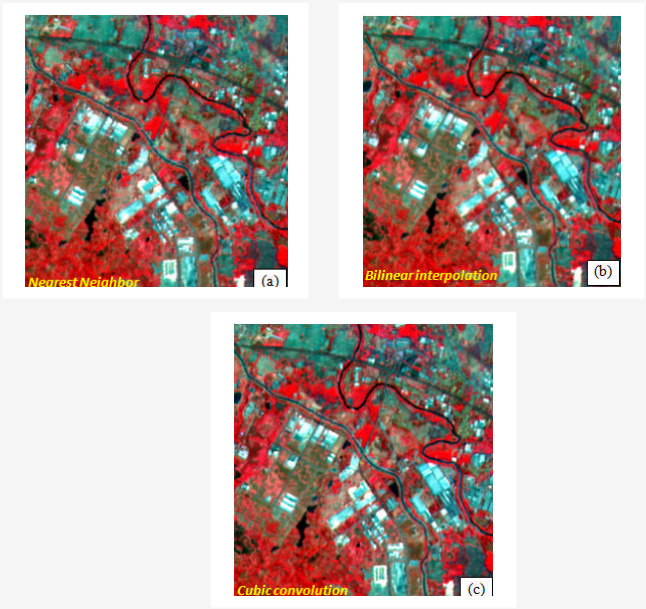

Fig. 18 The result of resampling the D2 configuration, (a) nearest neighbor, (b) bilinear interpolation, (c) cubic convolution

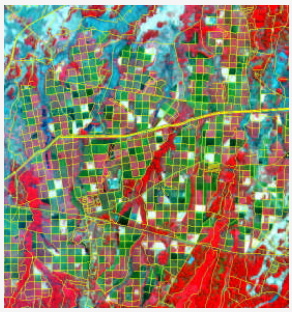

Fig. 19 Results cubic convolution resampling overlay with vector data path and the river RBI 1:25.000

Fig. 20 is one side of the cubic convolution resampling results from D2 configuration. The picture contains two strips dimosaik image manually. Almost every element on the border strip looks constantly, both on elements of buildings, rivers, roads and agricultural land parcels. Border or strip scene would look better going longer if using a mosaic assembly automatically and will help save time and effort in a project that consists of many images.

Fig. 20 Mosaic cubic convolution resampling results from D2 configuration, the dashed yellow line indicates the border strip.

IV. Conclusion

1. Accuracy ortho imagery products generated through triangulation of satellite imagery will be determined by the amount and distribution of GCP and TP. The more tightly the number of GCP and TP at regular intervals, the higher the resulting accuracy. Increasing the number of TP on sidelap and overlap will result in a better accuracy compared with the addition of GCP. TP usage will also save the use of GCP, so overall it will save effort should be spent.
2. Produced the highest accuracy of GCP configuration with a third distribution of the appropriate scene for a map scale of 1: 65,000. While most low accuracy is obtained from the GCP configuration without using a minimal amount of TP that only produce the map scale 1:116.000. The use of GCP distribution on the perimeter of the block alone is not recommended for triangulation of satellite imagery if not equipped with the TP.
3. The use of image stich will greatly help reduce the number of GCP and TP if conditions allow the image scene and equipped with ephemeris data.

V. Suggestion

1. This study has not yet reached the configuration GCP / TP saturated for triangulation SPOT4/SPOT2 satellite imagery by producing the highest accuracy. There are still opportunities to increase the number and density of GCPs more from D configuration, thus achieved the highest statistical accuracy.
2. Panchromatic image of SPOT4/SPOT2 not included in this study, so it needs to be further investigated whether enough with registration or required orthorectification itself in the image.

ACKNOWLEDGMENT

We would like to thank the leadership of the institution, associate in research that has helped the completion of this research activity. May be useful for those who read it

REFERENCES

[1] Arief, M., Kustiyo dan Surlan (2008). Kajian Ketelitian Koreksi Geometrik Data SPOT Level 2A; Studi Kasus Nusa Tenggara Timur, *Prosiding PIT MAPIN XVII*, Bandung 10-12-2008, 281 – 285.

[2] Baillarin, S., Bouillon, A. dan Berdnard, M. : Using a Three Dimensional Spatial Database to Orthorectofy Automatically Remote Sensing Images, *ISPRS Workshop on Service and Application of Spatial Data Infrastructure*, XXXVI (4/W6), Oct.14-16, Hangzhou, China (http://130.75.85.12/html/aktivitaeten/EARSeL-Workshop2005_Paper /Baillarin.pdf: diakses pada 15 November 2007)

[3] EC–JRC ISPRA (2008): *Guidelines for Best Practice and Quality Checking of Ortho Imagery***;** Issue 3.0. Post: IPSC-MARS, Institute for the Protection and Security of the Citizen, Monitoring Agriculture with Remote Sensing Unit, First issued: Ispra TP 266, Joint Research Centre, I-21020 Ispra (VA), Italy. (http://www.jrc.ec.europa.eu/ and http://ipsc.jrc.ec. europa.eu/: diakses pada 30 April 2009)

[4] FGDC-STD-007 (1998): *Geospatial positioning accuracy standards, Part 3: National Standard for Spatial Data Accuracy*, FGDC, Washington , D.C. (http://www.fgdc.gov/standards/projects/FGDC-standardsprojects/accuracy/part1/ index_html/?searchterm=Geospatial%20positioning%20 accuracy%20standards: diakses pada 15 Desember 2009)

[5] GAEL Consultant, (2004): *GAEL-P135-DOC-001, revision 4, 20/08/2004; SPOT 123-4-5 Geometry Handbook.* (http://www.spotimage.fr/automne_modules_files/standa rd/public/p229_0b9c0d94a22e77aac09df2b360c73073SP OT_Geometry_Handbook.pdf: diakses pada 25 Februari 2009)

[6] Gantini, T., Purba E. dan Purwoko (2008): Kajian Kualitas Posisi Geometri Data SPOT4, *Prosiding PIT MAPIN XVII*, Bandung 10-12-2008, 559 – 570.

[7] Ghilani, C.D. dan Wolf, P.R. (2008): *Elementary Surveying; An Introduction to Geomatics, 12th edition*. Pearson Prentice Hall, Pearson Education, Inc. Upper Saddle River, USA.

[8] Giannone, F. (2006): *A Rrigorous Model for High Resolution Satellite Imagery Orientation*, PhD Thesis, University of Rome "La Sapienza" Faculty of Engineering, Roma.

[9] Haining, R.P. (2003): *Spatial Data Analysis; Theory and Practice*, Cambridge University Press, Cambridge-United Kingdom.

[10]Jan´ee, G. (2007): SPOT Mirror and Incidence Angles. (http://www.alexandria.ucsb.edu/~gjanee/spot/docs/angle s.pdf: diakses pada 27 Januari 2009)

[11] Leica Geosystem (2005): *ERDAS Field Guide, Chapter 8: Photogrammetric Concepts*, Geospatial Imaging-LLC, Norcross, Georgia.

[12] Maune, D.F. (2001): *Digital Elevation Model Technologies and Applications: The DEM User Manual*, American Society of Photogrammetry and Remote Sensing, Bethesda, Maryland USA.

[13] Mikhail, E.M., Bethel, J.S. dan McGlone, J.C. (2001): Introduction to Modern Photogrammetry, John Willey & Sons, Inc., New York USA.

[14] Müller, R., Krauß, T., Lehner, M. dan Reinartz, P.: *Automatic Production of a European Orthoimage Coverage within The GMES Land fast Track Service Using* SPOT4*/5 and IRS-P6 LISS III Data*, German Aerospace Centre (DLR), Remote Sensing Technology Institute, D-82234 Wessling, Germany. (http://www.ipi.uni-hannover.de/fileadmin/ institut/pdf/Mueller_krauss_lehner_reinartz.pdf: diakses pada 8 Desember 2007)

[15] PCI Geomatics, (2006): *PCI Geomatica V10.0.3 help*, PCI Geomatics Enterprises Inc. 50 West Wilmot Street, Richmond Hill Ontario, Canada, L4B 1M5.

[16] Sari, I. L., Purwoko dan Kartasasmita, M. (2008): Koreksi Geometri Level 2B Data SPOT Bersudut (Pandang) Sensor Kecil, *Prosiding PIT MAPIN XVII*, Bandung 10-12-2008, 232 – 237.

[17] Schowengerdt, (2007): *Remote Sensing; Models and Methods for Image Processing, 3rd edition*, Academic Press, Elsevier Inc., USA.

[18] Tonon, M. (2005): *SPOT 5 data for line map updating: New perspectives in mapping.* (http://www.gisdevelopment.net/technology/survey/me0 5_122.htm: diakses pada 20 Februari 2009)

[19] Toutin, T., Carbonneau, Y. dan Chénier, R. (2001): Block adjustment of Landsat-7 ETM+ images, *ISPRS Joint Workshop, High Resolution from Space*, Hanover, Germany, September 19-21, 2001. (www.photogrammetry.ethz.ch/general/persons/jana/ispr s/tutmapup/ISPRS_tutorial_Toutin_hannover3.pdf: diakses pada 5 Maret 2009)

[20] Willneff, J. dan Poon, J. (2006): Georefencing from orthorectified and non-orthorectified high-resolution satellite imagery, *13th Australasian Remote Sensing and Photogrammetry Conference*, Canberra, Australia. (http://www.crcsi.com.au/uploads/136eae58-aaf6-4deb-a74b-34e3e6096ade/docs/ WillneffPoonCanberra2006.pdf: diakses pada 27September 2007)

[21] Wolf, P.R. dan Dewitt, B.A. (2000): *Elements of Photogrammetry; with Applications in GIS, 3rd edition*, McGraw-Hill Company, Inc., New York.

[22] Wolf, P.R. dan Ghilani, C.D. (1997): *Adjustment Computations; Statistics and Least Square in Surveying and GIS*; 3rd edition, John Wiley & Sons,Inc., Hoboken-New Jersey, Canada.

[23] Wolf, P.R. dan Ghilani, C.D. (2006): *Adjustment Computations; Spatial Data Analysis*; *4th edition*, John Wiley & Sons,Inc., Hoboken-New Jersey, Canada.

[24] Wolniewicz W. dan Chinh Ke L. (2006): *Geometric modelling of VHRS Imagery*. ISPRS International Calibration and Orientation Workshop EuroCOW 2006, 25-27 January 2006, WG I/3, Castelldefels, Spain. (www.isprs.org/commission1/euroCOW06/euroCOW06_files/papers/Geometric%20models%20-%20wolniewicz.doc: diakses pada 20 Februari 2009)

[25] Spot Image (2003a): SPOT Technical Information; Spot on its orbit. (http://www.spotimage.fr/automne_modules_files/standard/public/p229_fileLINKEDFILE_Spo-on-its-orbit.pdf: diakses pada 13 Agustus 2004)

[26] Spot Image (2003b): SPOT Technical Information; The Spot Payload. (http://www.spotimage.fr/automne_modules_files/standard/public/p229_file LINKEDFILE_Spot_payload.pdf: diakses pada 13 Agustus 2004)

[27] Spot Image (2003c): SPOT Technical Information; Image Acquisition. (http://www.spotimage.fr/automne_modules_files/standard/public/p229_fileLINKEDFILE_images-acquisition.pdf: diakses pada 13 Agustus 2004)

[28] Spot Image (2003d): Spot Image Product guide; Spot Image Products and Solutions. (http://www.spotimage.fr/automne_modules_files/standard/public/p222_fileLINKEDFILE1_Catalogue_SI-E.pdf: diakses pada 12 Maret 2009)

[29] Spot Image (2003e): SPOT Technical Information; Preprocessing levels and location accuracy. (http://www.spotimage.fr/web/en/234-preprocessing-levels-and-location-accuracy.php, p234_fileLINKEDFILE2_pretraitement-localisation-E.pdf: diakses pada 21 Juli 2004)

[30] Spot Image (2005[f]a): SPOT Technical Information; Resolutions and spectral modes. (http://www.spotimage.fr/web/en/233-resolution-and-spectral-bands.php, 233_1bbabf31105a2cf49217f6ce79596d0cres_modes_E.pdf: diakses pada 12 Maret 2009).

[31]Spot Image (2005[g]b): SPOT Technical Information; SPOT Satellite Technical Data. (http://www.spotimage.fr/automne_modules_files/standard/public/p229_3a1cd2cb59b76fc75e20286a6abb7efesatSpot_E.pdf: diakses pada 12 Maret 2009)

[32] Spot Image (2005[h]c): SPOT Technical Information, SPOT Satellite Programming a Custom Service. (http://www.spotimage.fr/automne_modules_files/standard/public/p230_97114bc824a947c5af8914cdf4b351edprog_E.pdf: diakses pada 27 September 2007)

[33] Spot Image (2008): SPOT Technical Information; Preprocessing levels and location accuracy. (http://www.spotimage.fr/automne_modules_files/standard/public/p234_0916b39e58c710b3bb5788fdcc025f80niveau_anglais_2008.pdf: diakses pada 12 Maret 2009) http://www.spotimage.fr/web/en/234-preprocessing-levels-and-location-accuracy.php: diakses pada 21 Juli 2004.